Annals of Arid Zone 64(4): 567-588, 2025

Quantitative Analysis and Mapping of Morphometric Characteristics and Water Erosion in the Watersheds of the Mediterranean Region: Application to the Case of Northern Algeria

Bellout Mahieddine* and Boutoutaou Djamel

Laboratories Exploitation and Valorization of Natural Resources in Arid Zones, University Kasdi-MERBAH Ouargla, Route de Ghardaïa BP 511 Owargla 30000 Algeria

Received: July 14, 2025 Accepted: August 5, 2025

Abstract: Water erosion, a complex and widespread phenomenon in the Mediterranean region—particularly in northern semi-arid Algeria—is the primary cause of soil degradation. It also impacts water quality and accelerates the silting of dams. This study utilizes data provided by the National Agency for Hydraulic Resources, covering 132 hydrometric stations. Analysis of liquid and solid discharges indicates that the power model is most suitable for assessing water erosion across different temporal scales. The average annual specific erosion varies among watersheds, generally ranging from 0.11 to 59.78 t·ha^{-1} yr^{-1}. The monthly distribution of solid inputs reveals that autumn is the peak season for solid transport in most studied watersheds, accounting for 38.93% of the total volume. Winter follows with a significant contribution of 28.27%, while spring accounts for 25.26%. Conversely, summer exhibits the lowest flows, representing only 7.54% of the total transport. Principal Component Analysis (PCA) enabled the classification of four hydrologically homogeneous groups. Subsequently, multiple regression analyses were conducted within these groups to identify a log-linear (Poisson) relationship between specific erosion and various explanatory variables, primarily the morphometric characteristics of the watersheds. Mapping the spatial distribution of specific erosion in northern Algeria serves as a vital tool for identifying the most erosion-prone areas. By providing a detailed assessment of at-risk zones, this mapping offers a clear guide for prioritizing intervention strategies in vulnerable sectors.

Key words: Water erosion, quantitative analysis, morphometric characteristics, mapping, watersheds, Algeria.

***Correspondence**
Bellout Mahieddine
belloutmahieddine@yahoo.fr

Citation
Mahieddine, B. and Djamel, B. 2025. Quantitative analysis and mapping of morphometric characteristics and water erosion in the watersheds of the mediterranean region: Application to the case of northern Algeria. Annals of Arid Zone 64(4): 567-588

https://doi.org/10.56093/aaz.v64i4.168990

https://epubs.icar.org.in/index.php/AAZ/article/view/168990

Water erosion represents a major environmental issue that affects vast regions on a global scale, particularly agricultural areas. Since 1930s, scientific research has deepened the understanding of this phenomenon, thereby facilitating its quantification and modelling in different contexts. This geographical and environmental phenomenon generates impacts whose magnitude and severity vary considerably from

one site to another. The variability, results from a combination of natural and anthropogenic factors, which influence the intensity and consequences of the phenomenon.

The causes of water erosion are complex and multifactorial. On the one hand, natural factors such as topography, soil composition, vegetation, and climate play an important role in soil vulnerability (Morgan, 2005). On the other hand, human activities—such as deforestation, unsustainable agricultural practices, and soil overexploitation—have intensified the phenomenon of water erosion (Pimentel *et al*., 1995). Extreme weather events linked to climate change increase the frequency and intensity of precipitation, contributing to the worsening of water erosion (FAO, 2001). The GLASOD (Global Assessment of Human-Induced Soil Degradation) survey highlighted a concerning reality: approximately 15% of the world's land is affected by physical soil degradation, endangering not only agricultural productivity but also ecological balance (Oldman *et al*., 1991). Furthermore, it is estimated that nearly 36 billion tons of soil are eroded each year globally. This phenomenon is mainly attributed to water erosion and human practices such as intensive agriculture and deforestation (FAO, 2001). The economic consequences of soil erosion are not negligible: according to projections, economic losses due to the decrease in agricultural productivity could reach 625 billion dollars by 2070 (JRC, 2024). According to the FAO, 2020, approximately 30% of agricultural land in the Mediterranean region is exposed to degradation risks, primarily due to water erosion. This phenomenon can lead to annual soil losses ranging from 12 to 40 t ha^{-1} (Lal, 2001). It also constitutes a significant characteristic of the Maghreb region, where water and soil resources are severely threatened (Touaïbia *et al*., 2001; Terfous *et al*., 2001; Achit and Meddi, 2005; Semari and Korichi, 2023). In Morocco, the annual cumulative loss of land is estimated at 100 mt. In Tunisia, water erosion affects 8.5 mha, representing 52% of the country's total area (Semari and Korichi, 2023). In Algeria, 45% of the Tellian region is affected, which is approximately 12 mha, of which 6 m ha are currently subjected to active erosion (Zeggane and Boutoutaou, 2016).

Numerous studies have attempted to quantify water erosion in our country (Medfouni *et al*., 2024; Fredj *et al*., 2024; Mrad *et al*., 2024; Fellah *et al*., 2024; Toubal *et al*., 2024; Chaïeb *et al*., 2024; Aouadj *et al*., 2023; Bensekhria and Bouhata, 2023; Zekri and Tounkob, 2021; Ghernaout and Remini, 2017; Zeggane, 2017; Bouanani *et al*., 2013; Elahcene *et al*., 2013; Achit and Meddi, 2005; Bouanani, 2004; Megnounif *et al*., 2003; Terfous *et al*., 2001; Meddi, 1992; Bourouba, 1997; Demmak, 1982; Sogreah, 1967), but these studies face methodological limitations, such as the lack of reliable local data and the use of models poorly suited to the specificities of each watershed. This gap makes it difficult to accurately estimate specific erosion and solid transport, particularly in a diverse geographical and hydrological context.

The insufficiency, or even the absence, of solid discharge measurements on the majority of rivers in Algeria complicates the collection of essential data on solid transport, making it difficult to assess this phenomenon accurately. This situation creates additional challenges for professionals, who often find themselves working without reliable data or clear normative documents. Given this lack of data and the necessity to adopt a regional and specific approach, it becomes imperative to propose an innovative methodology capable of estimating solid transport and assessing soil degradation in these particular watersheds. This study aims to develop a methodology to assess solid transport in ungauged watercourses and to create an erosion map for the northern region of Algeria. Engineers and planners in the field of hydraulics will often use the results obtained, often deprived of measurement data and normative documents.

Material and Methods

Geographical and climatic overview of the study area in northern Algeria

The research focuses on the watershed in the northern part of Algeria, covering approximately 365000 km² and forming the central region of the Maghreb. It stretches about 350 km from north to south and nearly 1000 km along the Mediterranean coastline. To the west, it borders Morocco, while Tunisia lies to the east. The Mediterranean Sea forms the northern boundary, and the southern slopes of the Saharan Atlas define the southern boundary (Fig. 1). Algeria's territory is divided into two central geographical regions: the coastal strip,

which is 200 to 300 km wide and has a 1200 km long coastline, and the vast Saharan region to the south.

The area exhibits significant climatic diversity. The northern part has a Mediterranean climate, with mild, wet winters and hot, dry summers, while the southern region transitions into a sub-desert climate characterized by arid conditions and considerable temperature fluctuations. Geologically, the region is complex, featuring various formations ranging from permeable to highly permeable, as well as semi-permeable and impermeable. This geological diversity greatly influences the distribution of surface water. The northern region is a key reservoir for the country's surface water resources, housing the necessary hydraulic infrastructure for their management and use. In contrast, the southern part of Algeria relies predominantly on groundwater resources, particularly from the Albian aquifer, which serves as the primary water source for the region.

Sources of data

The study is conducted using data collected by the National Agency for Hydraulic Resources of Algeria at 132 hydrometric stations (Fig. 2). These data include instantaneous liquid flow rates (m^3s^{-1}) and instantaneous suspended sediment concentrations (gl^{-1}) collected during the flood period at time interval of, 30 minutes. The traditional method of measuring liquid flows relies on the use of a regularly checked and updated calibration curve, allowing the conversion of water heights read on a limnimetric scale or extracted from the recordings of a float limnigraph. Regarding the sediment concentration, at each water level reading, a sample of turbid water is taken at a single point on the bank, at the surface of the stream, using a 50 cl bottle. The sediments filtered through a filter paper (0.45 µm) are then dried in an oven for 24 hours at a temperature of 105 °C. Once brought to a unit volume (1 litre), this load is attributed to the concentration of suspended matter carried by the watercourse, expressed in gl^{-1}.The number of samples and their correct temporal distribution determine the reliability and accuracy of the power relationship between the solid flow rate and the liquid flow rate.

Morphological parameters of the watersheds selected for the study

The traditional methods used for studying the physical complex of a watershed mainly rely on manual approaches, whose results are often less reliable. However, with the emergence of advanced technologies such as remote sensing and geographic information systems (GIS), it is now possible to define all the

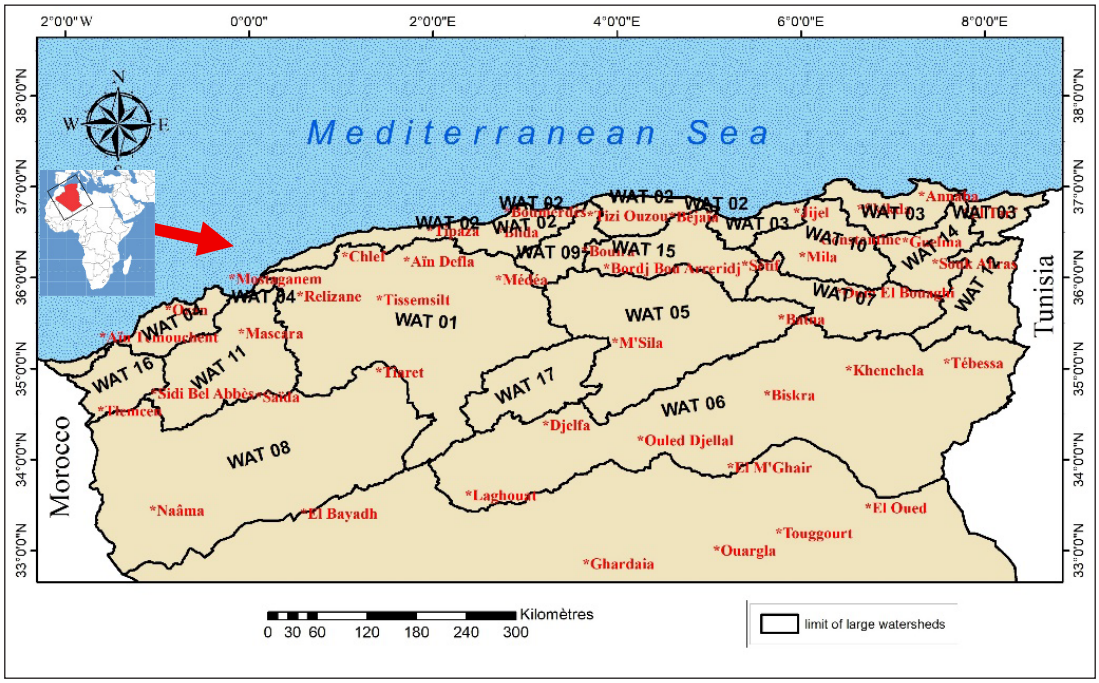

Fig. 1. The study area.

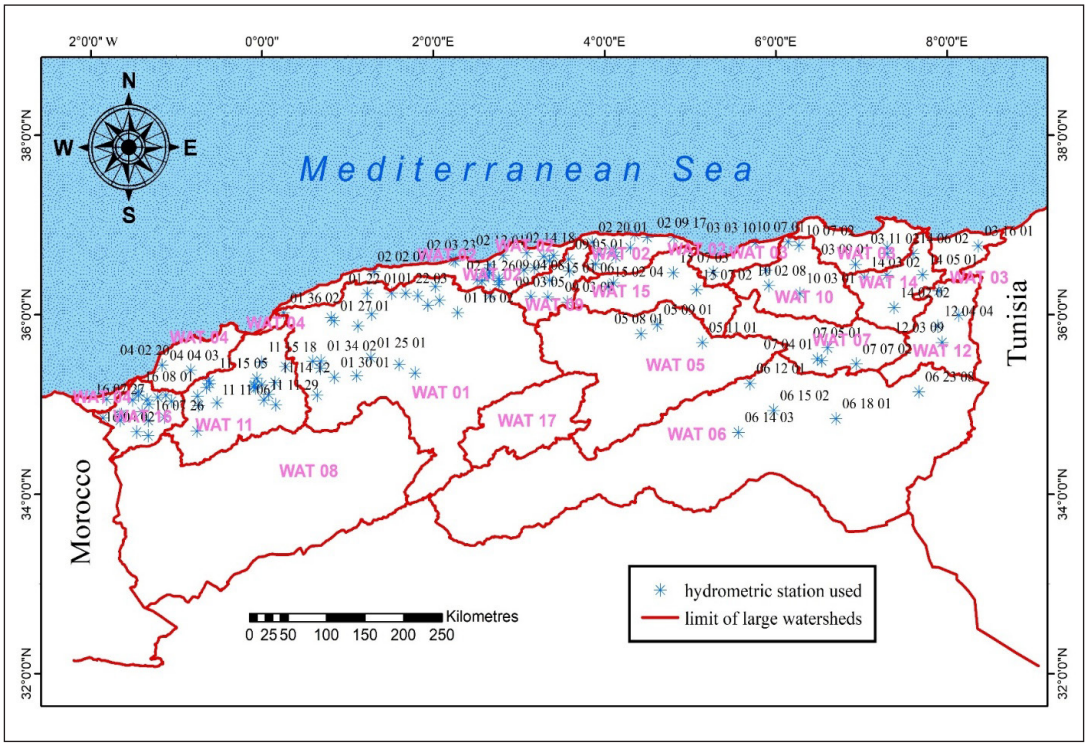

Fig. 2. The geographical distribution of the 132 hydrometric stations used in the study.

morphological and environmental parameters of the watershed with great precision and in detail. These modern tools not only overcome the limitations of classical methods but also provide more reliable and comprehensive information, thus facilitating a thorough assessment of the watershed's characteristics and its hydrological behavior.

The delineation of the 132 watersheds and the determination of their characteristics were carried out using ArcGIS 10.3 software, utilizing the digital elevation model (DEM). This process allowed for the precise mapping of the contours and boundaries of the watersheds, integrating detailed topographic data from the DEM. The use of this technology facilitated the analysis of various geomorphological parameters such as slope, altitude, and basin shape, which are essential for understanding local hydrological dynamics. Moreover, GIS has made it possible to associate this spatial information with other environmental and hydrological data, thus providing a comprehensive and integrated view of each watershed with a precision far superior to that of traditional manual methods.

Analysis of relation between liquid flow and solid flow at different time scales

In the field of solid sediment transport research, analyzing the relationship between the concentration of suspended particles and the liquid flow rate in a watercourse is essential for understanding hydrodynamic mechanisms and predicting environmental impacts, such as reservoir siltation or pollution of aquatic ecosystems. Instantaneous measurements of liquid and solid flows allow for the study of their interconnection over different time scales, ranging from instantaneous to daily, monthly, and annual. The main objective is to develop regression models capable of predicting the transport of solid particles based on the liquid flow rate, taking into account seasonal variations. The most commonly used regression models for this purpose are the power, linear, logarithmic, exponential and parabolic model.

Estimation of specific erosion

Specific degradation refers to the amount of soil eroded per unit area and per unit time, generally expressed in tons per square kilometer per year (t km^{-2} yr^{-1}) or tons per hectare per year (t ha^{-1} yr^{-1}). It is a key indicator for quantifying erosion intensity within a given watershed and for comparing degradation levels across different regions (Roose *et al.*, 2005).

The evaluation of specific degradation, or specific erosion, constitutes an essential indicator for assessing the erodibility of each region, thus providing crucial information on the vulnerability of storage structures to the risk of siltation. This analysis is essential to anticipate the impact of erosion on hydraulic infrastructures and better manage the associated risks. It is important to emphasize that the absence of direct measurements prevents an accurate quantification of bed load transport. Due to this gap, the present study adopts an indirect approach by estimating bedload transport based on an average corresponding to 20% of the suspended load, in accordance with observations made in some areas of the Maghreb (Touaïbia *et al*., 2003).

Multivariate analysis of specific erosion

The objective of multivariate analysis is to model the joint distribution of multiple variables, taking into account both the individual variations of these variables and the correlations between them. This approach aims to develop a specific erosion model for each group based on various morphometric, climatic, geological, and biophysical parameters (such as topography, vegetation cover, etc.) expressed in t ha^{-1} yr^{-1}. The spatial model thus obtained will allow for the estimation of specific erosion at any point in the watersheds of northern Algeria.

The statistical method of multiple regressions enables the prediction of an individual's score on a single variable by considering their scores on many other factors.

Consider a random sample of n observations (x i1, x i2, ... , x ip, y i), i = 1, 2,3, . . . , n

The p + 1 random variables are assumed to satisfy the linear model:

yi = β0 + β1 x i1 + β2 x i2 + βp x ip + ui; i = 1,2,3, . . . , n.

Where ui are values of an unobserved error term, u, and the unknown parameters are constants. The overall goodness of fit of the regression model (i.e., whether the regression model is at all helpful in predicting the values of y can be evaluated, using an F-test in the format of analysis of variance) (Sureiman and Mangera, 2020).

Specific erosion mapping

This spatialized approach allows for the visualization, analysis, and better understanding of the spatial variability of erosion across the entire watershed in northern Algeria. The map thus produced will highlight the area's most vulnerable to erosion, facilitating the identification of priority sectors where targeted interventions will be necessary.

Mapping involves the use of different interpolation methods to estimate the values of unknown variables from data measured at specific points. The choice of interpolation method depends on the nature of the available data, the purpose of the map, and the required level of precision. Among the primary spatial interpolation methods commonly used in cartography, we find Interpolation using the Inverse Distance Weighting method (IDW – Inverse Distance Weighting), Kriging Interpolation, Spline Interpolation, Trend Surface Analysis, Natural Neighbor Interpolation, Thiessen Interpolation; Interpolation by moving average.

Results and Discussion

Characteristics of the basins at gauging stations

Table 1 presents the morphometric characteristics of a subset of the 132 watersheds examined in this study. The analysis of the 132 studied watersheds highlights a tremendous physical, topographical, and morphometric diversity, reflecting the variety of geographical contexts encountered. The areas vary considerably, ranging from 5.52 km^2 for the smallest basin (W 16 06 11) to 43 952.76 km^2 for the largest (W 01 36 02), reflecting a wide range of hydrological scales. The compactness coefficient (Kc) ranges from 1.19 to 2.49, with an average between 1.65 and 1.70. Approximately 80% of the basins exhibit values between 1.40 and 1.90, indicating predominantly moderately compact to moderately elongated shapes. Some basins are distinguished by a particularly compact shape (W 16 06 11) or a very elongated shape (W 06 14 03, W 12 04 01), which can influence the dynamics of floods. The following maps (Figs. 3–7) illustrate specific features of some watersheds selected from the 132 studied.

The general topography of the basins is highly varied. The minimum altitude ranges from 4 m (W 02 08 08), suggesting coastal or

Table 1. Overview of the characteristics of certain watersheds, selected from the total of 132 monitored at gauging stations in the study area

Station code	Parameters												
	A	P	GI	H_{max}	H_{min}	H_{mean}	$H_{5\%}$	$H_{95\%}$	AS	L_{mw}	ASW	Dd	Ct	Tc
01 20 01	26 585.93	1 338.60	2.30	1 803	163	876.75	1 315	449	10.65	565.04	0.70	4.17	35.05	70.17
01 34 02	5 411.78	458.80	1.75	1 338	208	864.04	1 213	433	11.44	153.00	1.06	4.11	35.05	25.56
01 36 02	43 952.76	1 705.20	2.28	1 960	10	758.58	1 237	164	12.44	743.44	0.67	4.10	34.17	89.26
02 03 01	217.06	87.27	1.66	1 415	15	401.66	1 048	54	29.69	35.14	2.72	2.95	16.99	7.10
02 10 01	153.55	64.55	1.46	1 209	232	536.47	825	318	23.32	26.15	1.93	3.10	17.12	6.36
03 16 01	675.78	153.51	1.65	1 189	33	398.53	829	71	19.05	49.52	2.05	3.40	21.40	11.66
04 01 01	100.62	54.33	1.52	1 116	61	366.69	829	127	21.54	18.99	3.93	2.96	15.19	4.90
05 09 01	1 337.76	211.62	1.62	1 885	651	1 080.34	1 490	812	13.56	82.05	1.29	3.31	18.47	16.25
06 14 03	24 610.28	1 394.93	2.49	1 711	61	760.16	1 282	196	8.36	530.27	0.81	2.77	9.89	67.27
07 05 01	763.41	167.60	1.70	2 319	879	1 272.81	1 762	930	16.03	69.63	1.68	3.41	19.49	13.54
09 01 01	664.85	148.27	1.61	1 466	591	947.67	1 197	704	16.00	57.17	1.26	3.19	17.23	12.50
10 02 08	174.53	70.61	1.50	1 371	626	949.15	1 181	693	22.01	22.95	2.39	3.05	17.00	6.07
11 01 01	961.47	185.57	1.68	1 452	927	1 165.75	1 276	1 032	7.44	66.38	0.93	3.53	20.76	18.09
11 10 03	2 597.32	385.68	2.12	1 473	298	966.01	1 309	569	9.86	157.30	0.99	3.42	19.83	21.27
12 04 01	4 544.96	558.17	2.32	1 633	492	917.58	1 247	631	10.22	179.05	0.72	5.17	65.65	32.61
14 06 02	103.36	52.21	1.44	910	63	307.18	575	104	16.17	25.78	2.29	2.84	15.70	6.35
15 07 02	2 336.51	303.22	1.76	1 757	784	1 016.01	1 252	879	10.95	98.27	0.68	3.45	19.99	27.96
16 06 14	870.86	178.62	1.69	1 622	389	948.15	1 389	525	19.74	63.42	1.83	3.03	17.08	11.27
16 07 02	1 233.94	230.78	1.84	1 622	247	813.23	1 361	342	18.05	87.86	1.49	3.03	17.25	14.30

A: Area (km²); P: Perimeter (Km); GI: Gravelius Index; H_{max}: maximum altitude (m); H_{min}: altitude minimale (m); H_{mean}: mean altitude (m); $H_{5\%}$: Altitude matching 5% of the global area (m); $H_{95\%}$: Altitude matching 95% of the global area (m); L_{mw} : Length of main watercourse (km); AS: Watershed average slope (%); ASW: the average slope of the main watercourse (%); Dd : Drainage density (km/km²); Tc: Time of concentration (h); Ct: coefficient of torrentiality.

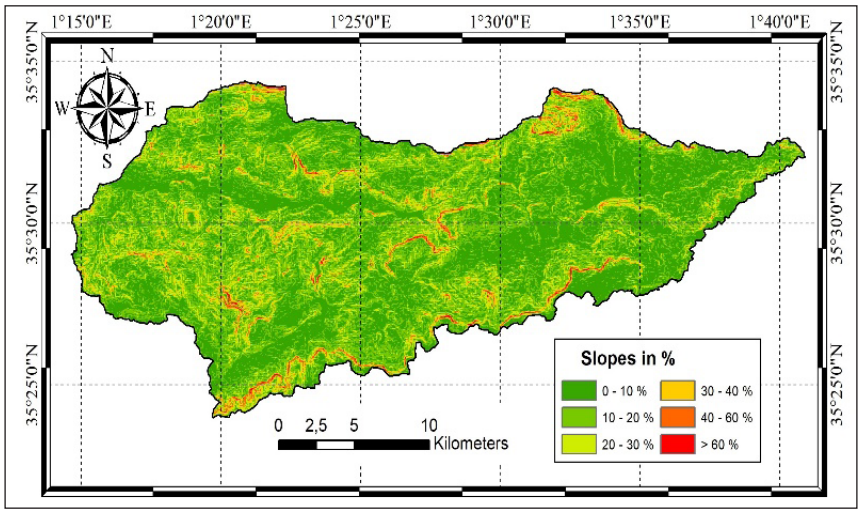

Fig. 3. Slope map of watershed 012501.

plain basins, to 1 129 m (W 16 07 26) for the highest areas. The maximum altitude reaches 2 321 m (W 06 18 01 and W 07 04 03), while the average altitude ranges between 149 m and 1 462 m. About one-third of the basins have an average altitude above 1 000 m, highlighting the predominance of mid to high mountain areas in the sample. These altitudinal variations directly influence the potential energy of runoff as well as erosive processes. The average slope (AS) of the basins, a key indicator of topographic roughness, varies from 5.47% (W 01 09 07) to 41.09% (W 02 17 15). Several basins exhibit slopes greater than 30%, often associated with intense runoff. The specific elevation difference, on the other hand, varies

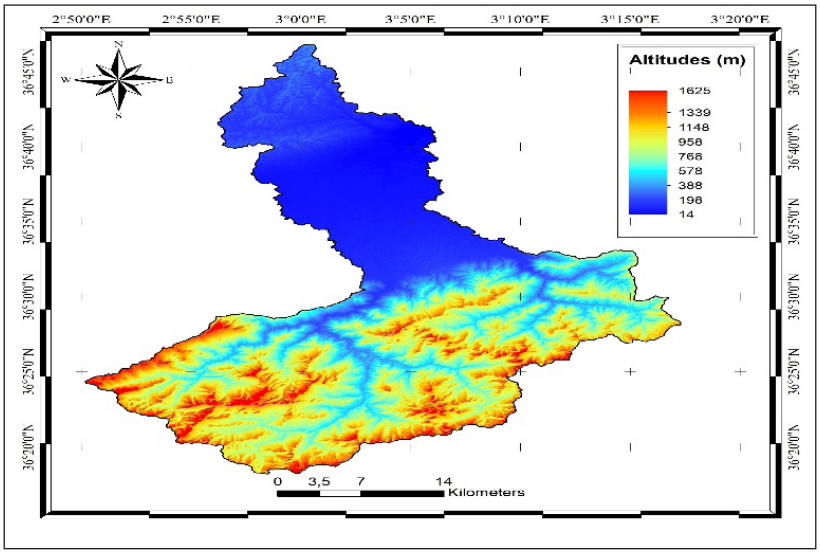

Fig. 4. Elevation map of watershed 021418.

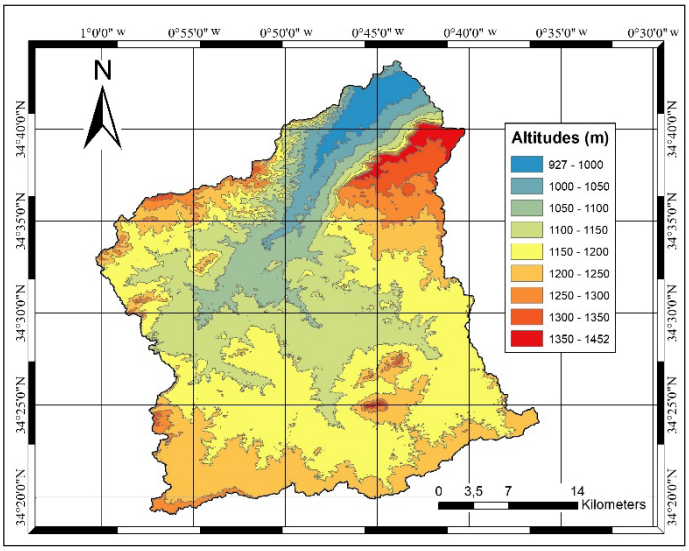

Fig. 5. Hypsometric map of watershed 110101.

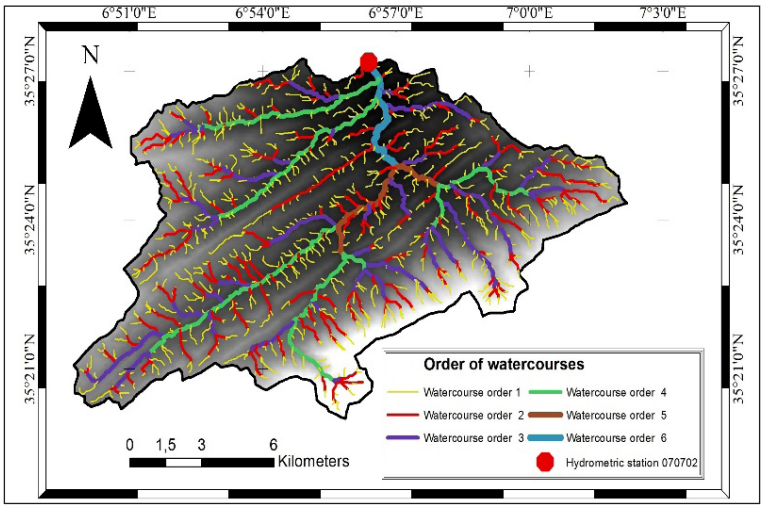

Fig. 6. Ordination of watercourses according to Trahler of watershed 070702.

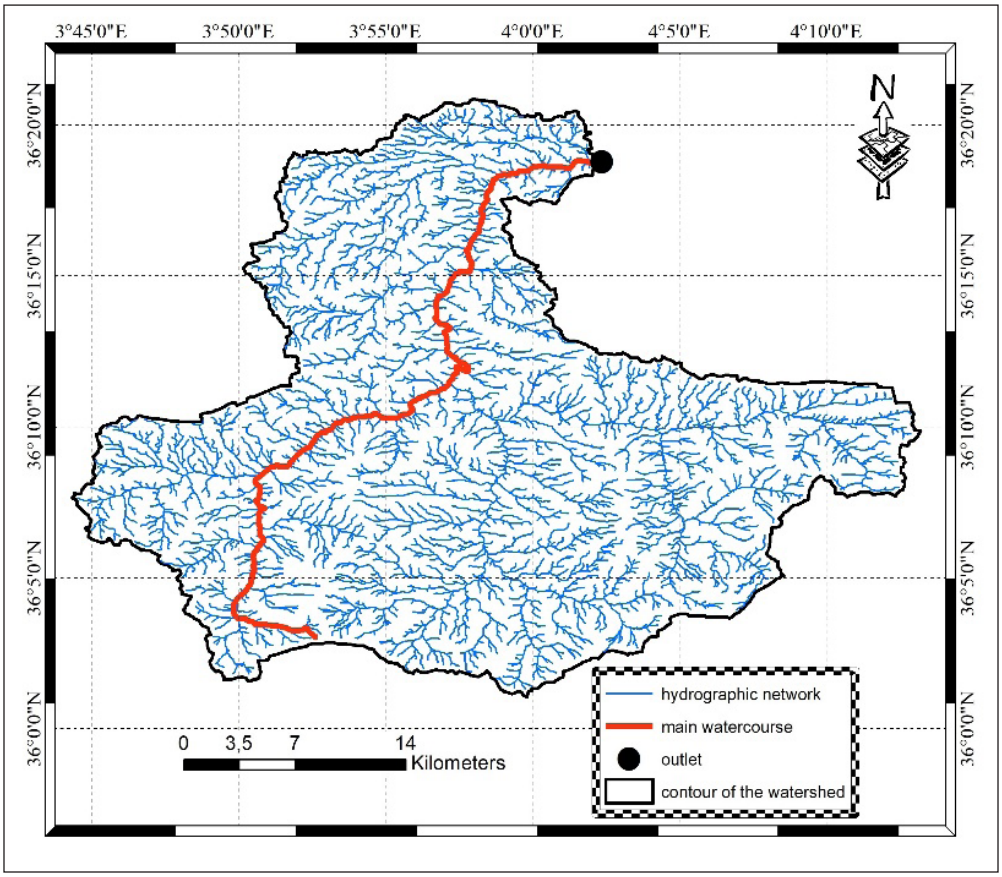

Fig. 7. The map of the hydrographic network and main waterways of watershed 150204.

from 71.13 m to 683.72 m. More than 60% of the basins show a Ds greater than 200 m, which confirms a generally marked relief and a strong gravitational drainage capacity.

From a hydro geomorphological perspective, the length of the main watercourse (Lmw) varies from less than 5 km to more than 740 km, while its average slope (ASW) ranges from 0.67% to 6.10%. The drainage density (Dd), generally greater than 3 km/km², indicates well-developed hydrographic networks. The torrentiality coefficient (Ct) shows very heterogeneous values, ranging from moderate to highly torrential. Finally, the time of concentration (Tc) varies from 2.4 hours to 89.3 hours, illustrating very contrasting flow dynamics depending on the morphology, slope, and shape of the watersheds.

Analysis of the relationships between liquid flows and solid flows at different time scales

Through the analysis of data from various hydrometric stations and at different temporal scales studied, the power-type model stands out as the most relevant, in accordance with the work of Dagnellie (1992), which relies on the coefficient of determination R^2. This trend is largely confirmed by several studies conducted in Algeria (Demmak, 1982; Benkhaled and Remini, 2003; Zeggane and Boutoutaou, 2016; Bouanani, 2004). Figure 8 and Table 2 illustrate the relationship between liquid and solid discharges at multiple temporal scales for a subset of watersheds in the study area.

On the whole of the data (instantaneous relationship), the graphical representation of solid and liquid flows (Fig. 8) highlights a substantial dispersion of points for the majority of the studied stations. This marked variability is explained by the influence of a complex set of factors on sediment concentrations (Asselman and Middelkoop, 2003). The sediment supply is remarkably variable, as it depends on several factors, including seasonal conditions and characteristics specific to the watershed, such as its antecedent state. Thus, sediment availability varies considerably from one season to another and is strongly influenced

Table 2. Calibrated models across various temporal scales, along with their corresponding coefficients of determination, for a subset of watersheds in the study area

Temporal scales	Variation of parameter "a"	Variation of exponent "b"	Selected model	Example for some watersheds		
				Station code	Determination coefficient (R^2)	Relationships retained
Instantaneous	0.08-85.39	0.79-1.91	Power: $Qs = a\ Ql^b$	013402	0.8499	$Q(s) = 10.004\ Q(l)^{1.2697}$
				031601	0.8309	$Q(s) = 0.2217Q(l)^{1.5205}$
				040220	0.8164	$Q(s) = 4.7146Q(l)^{1.8551}$
				050801	0.8995	$Q(s) = 9.4114Q(l)^{1.1866}$
Daily	0.02-46.46	0.93-2.68		061403	0.8305	$Q(s) = 4.9263Q(l)^{1.2828}$
				013302	0.8065	$Q(s) = 2.7086Q(l)^{1.7067}$
				070401	0.901	$Q(s) = 3.39Q(l)^{1.3206}$
				120309	0.9213	$Q(s) = 10.742Q(l)^{1.5205}$
Monthly	0.042-36.54	0.78-2.22		013001	0.8636	$Q(s) = 3.8449Q(l)^{1.475}$
				021201	0.8192	$Q(s) = 2.5196Q(l)^{1.1781}$
				070401	0.9041	$Q(s) = 3.3026Q(l)^{1.3635}$
				120309	0.8921	$Q(s) = 9.0018Q(l)^{1.2934}$
Annual	0.03-50.69	0.84-2.06		012701	0.8437	$Q(s) = 49.003Q(l)^{1.0741}$
				111403	0.8706	$Q(s) = 2.6051Q(l)^{1.1813}$
				150106	0.9681	$Q(s) = 0.0793Q(l)^{1.6109}$
				160202	0.806	$Q(s) = 1.5461Q(l)^{1.371}$

by extreme hydrological events, such as floods. These, particularly through their different phases (beginning, rise, fall), profoundly alter the conditions of sediment transport and deposition, which accentuates the dispersion observed in the data. These variations are all the more pronounced as local factors, such as land management practices and watershed development, also condition them. The regression analyses conducted using different functional forms showed that the power model is the most suitable, as evidenced by its generally higher coefficient of determination (R^2) (Table 2). This superiority of the power model reflects a better ability to explain the variability of the data compared to the other tested models. Regarding the model parameters, coefficient a shows a wide range of variation, from 0.08 to 85.39, while the exponent b varies between 0.79 and 1.91. This significant variability suggests that the relationships between the studied variables may differ considerably depending on the environmental and hydrological contexts specific to each watershed.

On a daily scale, the power model continues to stand out as the most effective among those evaluated in this study. The coefficients a and b of this model exhibit notable variability, ranging from 0.02 to 46.46 for a and from 0.93 to 2.68 for b, respectively. This wide range of values highlights the power model's flexibility and adaptability in the face of the diversity of hydrological conditions and the datasets analyzed.

The analysis of the results regarding the monthly scale correlation highlights a significant decrease in the dispersion of points, indicating improved reliability and increased consistency of the adjustments made to the data. This improvement is particularly well illustrated by the performance of the power model, which continues to stand out as the most effective among all the models studied. The variations observed in the parameters of the power model are remarkable. The parameter a, which varies from 0.042 to 36.54, indicates a wide range of applicability of the model. At the same time, the exponent b, which characterizes the exponential nature of the relationships, fluctuates between 0.78 and 2.22, highlighting complex and varied dynamics depending on the analyzed data. The relationships highlighted at this scale offer interesting perspectives, as they can be exploited in a wide range of scientific applications, particularly to deepen hydro sedimentary studies, refine predictive models, or even improve ecosystem management strategies. This robust performance underscores

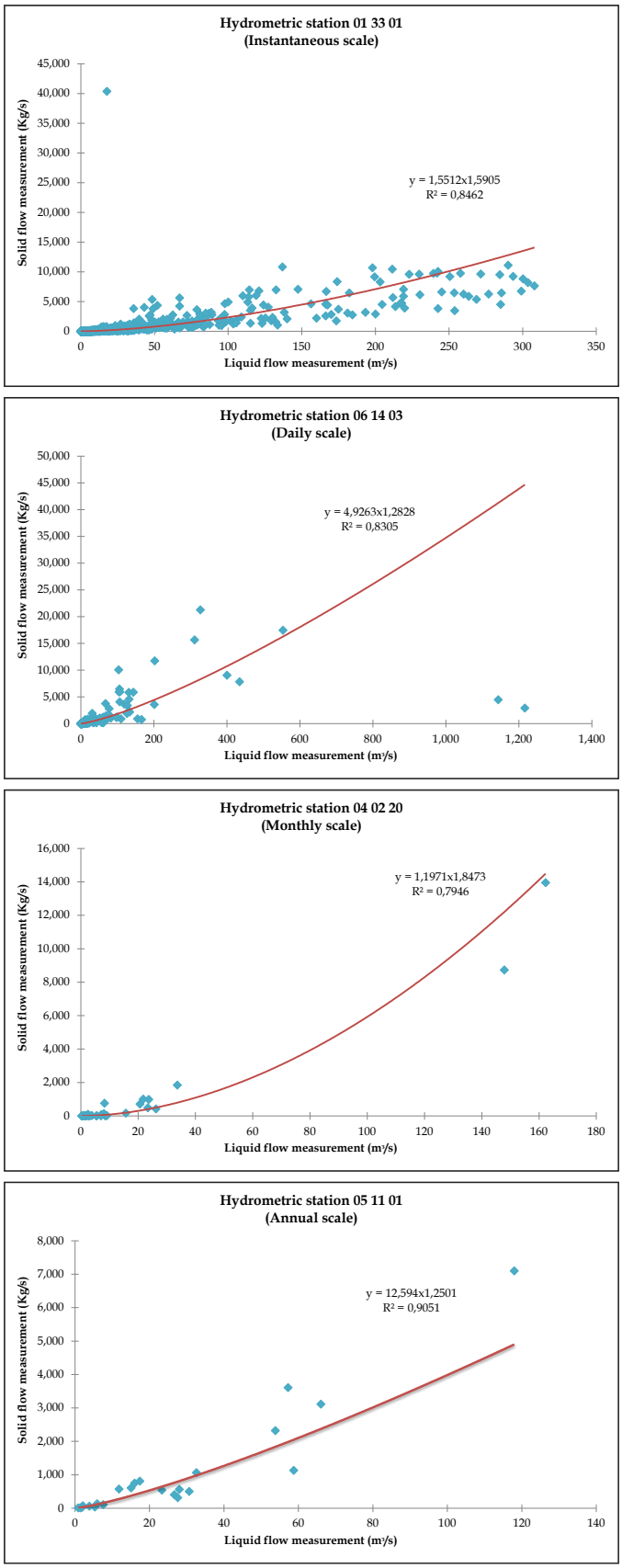

Fig. 8. Relationship between liquid and solid flows at different time scales for a subset of watersheds in the study area.

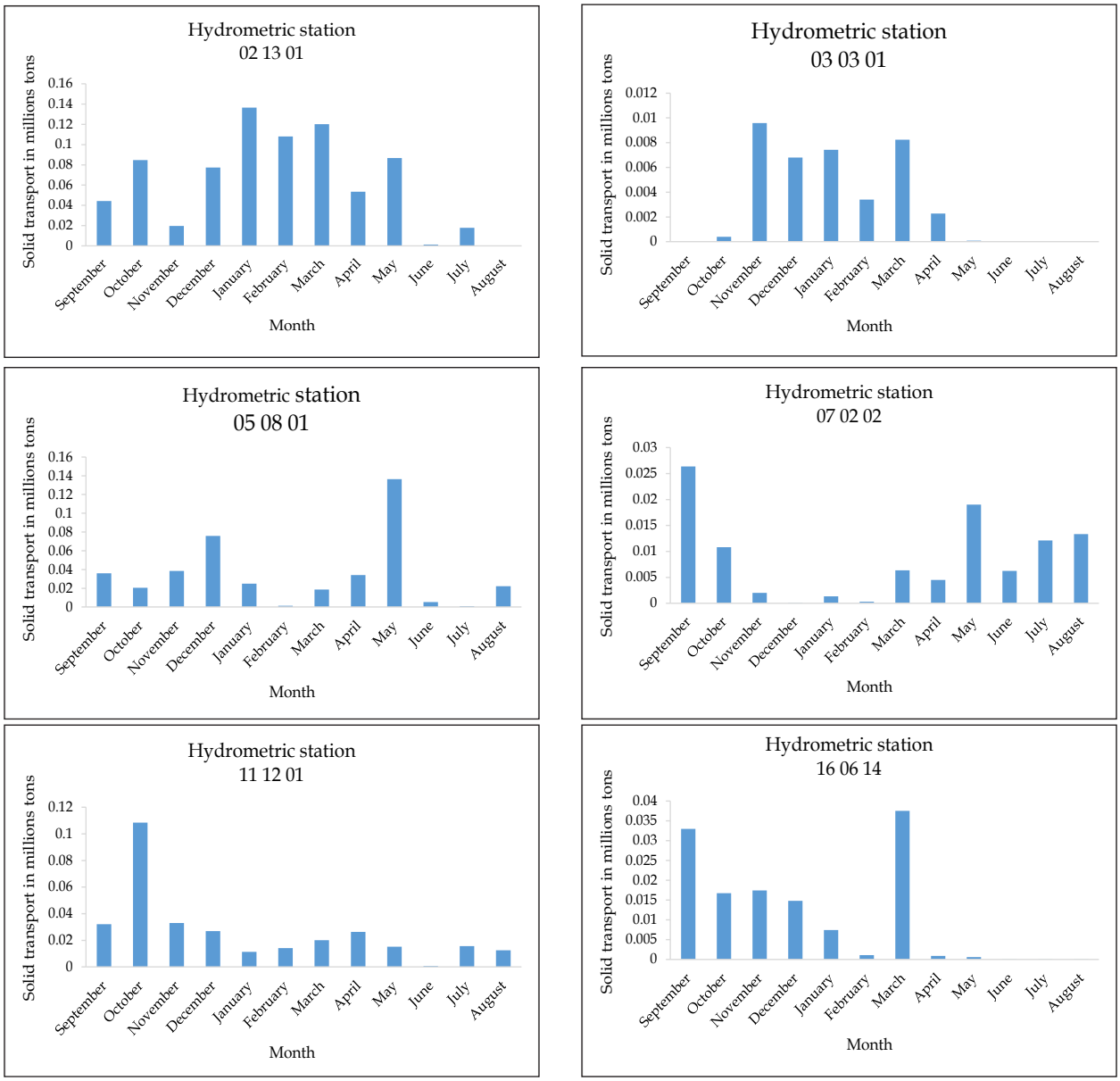

Fig. 9. Monthly variation of sediment yields in a subset of watersheds in the study area.

the importance of continuing research based on this model for future applications.

The detailed analysis of the results obtained on an annual scale highlights a dispersion of statistically insignificant points, which demonstrates the robustness of the models studied. Among these models, the power model stands out clearly, confirming its status as the most efficient model among all the advantageous approaches in this study. The parameters characterizing this model, namely the coefficient a and the exponent b, range respectively from 0.03 to 50.69 and from 0.84 to 2.06, reflecting its ability to adapt to various contexts. They present a strong potential for application and can be utilized in numerous subsequent studies, particularly in fields with precise and reliable modeling.

Monthly analysis of the distribution of solid inputs

Figure 9 illustrates, using histograms, the monthly distribution patterns of sediment inputs for a subset of watersheds in the study area.

The results obtained regarding the distribution of solid inputs on a monthly basis highlight significant temporal and spatial

Table 3. Assessment of specific erosion rates in a subset of watersheds within the study area

Station codes	Specific erosion (t ha^{-1} yr^{-1})	Station codes	Specific erosion (t ha^{-1} yr^{-1})	Station codes	Specific erosion (t ha^{-1} yr^{-1})
01 19 05	26.63	05 11 01	5.59	11 14 12	1.27
01 27 01	20.21	06 12 01	2.87	11 14 25	8.40
02 03 23	12.37	06 14 03	0.56	12 03 09	1.38
02 06 09	7.38	07 05 01	16.93	12 04 01	1.40
03 03 10	20.80	07 07 02	8.58	14 02 02	1.35
03 16 01	9.15	09 03 05	3.89	14 05 01	2.85
04 01 01	3.52	09 03 09	7.55	15 01 06	6.20
04 02 20	7.10	10 02 08	3.27	15 02 04	6.48
05 09 01	10.90	10 07 01	10.79	16 02 02	1.68

variation in solid transport across the different studied watersheds. A thorough analysis of the monthly data highlights notable fluctuations: the amount of sediment transported varies not only from month to month but also from one watershed to another, reflecting the influence of numerous local and climatic factors.

Autumn stands out as the season during which solid transport reaches its peak in the majority of the studied watersheds, accounting for 38.93% of the total volume. This seasonal peak far exceeds the levels observed during other times of the year, highlighting the decisive influence of the hydrological conditions specific to this season. Indeed, the abundant rainfall and autumn floods intensify soil erosion and thus promote sediment transport. After this period, the intensity of solid transport gradually decreases. Winter records a notable contribution of 28.27%, followed by spring with 25.26%, while summer is characterized by the lowest flows, representing only 7.54% of the total transport.

Estimation of the specific degradation rate

Specific erosion was determined for all the measurement stations, and the corresponding results for a number of them are grouped in Table 3.

The results reveal a high variability in specific degradation among the 132 studied watersheds. The values range from 0.11 t ha^{-1} yr^{-1} (Tafna Village) to 59.78 t ha^{-1} yr^{-1} (Ouled Fares), reflecting the combined influence of environmental (topography, climate, vegetation cover) and anthropogenic (land use, agricultural practices) factors. The average value, estimated at 8.21 t ha^{-1} yr^{-1}, indicates a generally high level of erosion. Spatially, erosion is more pronounced in the north, due to a wetter climate and more exposed soils, as well as in the east, characterized by rugged terrain and

Table 4. Results of the PCA

Component	Variance		Eigenvalue
	Proportion explained	Cumulative	
C1	61.60%	61.60%	7.39
C2	12.10%	73.70%	1.45
C3	8.00%	81.70%	0.96
C4	7.36%	89.06%	0.88
C5	3.63%	92.69%	0.44
C6	2.35%	95.04%	0.28
C7	1.74%	96.78%	0.21
C8	1.04%	97.82%	0.12
C9	0.78%	98.60%	0.09
C10	0.64%	99.24%	0.08
C11	0.40%	99.65%	0.05
C12	0.35%	100.00%	0.04

heavy rainfall. These areas thus appear to be particularly vulnerable.

Regionalization of sediment transport within the study area (northern Algeria)

A principal component analysis (PCA) was conducted to structure the data, summarize the variability between the stations, and establish a typology of hydrological regimes, highlighting the main trends in solid transport. The results are presented in Table 4 and illustrated in Figure 10.

The first principal component (C1) alone explains a significant proportion of the total variance, namely 61.6%. This result indicates that this component captures the essential information of the original variables. The addition of the second principal component (C2) increases the cumulative proportion to 73.7%, which suggests that the first two components are sufficient to represent a large majority of the data structure. The following components contribute decreasingly to the total variance. The third (C3) and fourth (C4) explain 8% and 7.36% of the variance, respectively, bringing the cumulative total to 89.06% after the first four components. This decreasing trend continues with C5 and beyond, where individual contributions become increasingly marginal. For example, the fifth component (C5) adds only 3.63% of the variance, and the sixth (C6) adds even less (2/35%). These values show that the components beyond C4 provide only a minor amount of additional information. Examining the associated eigenvalues, we find that they decrease rapidly, with a value of 7.39 for C1, dropping to 1.45 for C2, and then continuing to decrease to 0.04 for C12. This confirms that the majority of the information is concentrated in the first components.

When projecting the variables onto the two principal axes, it is observed that the first component, C1, highlights the seasonal variations in solid transport regimes. The stations negatively correlated with this component are characterized by low average annual solid discharge rates. Conversely, the stations positively correlated display relatively high annual solid discharge rates, indicating an intensification of sediment transport during the wet season. This component thus helps explain the "average" behavior of solid transport on an instantaneous scale, highlighting the temporal fluctuations of sediment flows.

Furthermore, the projection of the variables onto the second principal component, C2, reveals a spatial structuring of sedimentary flows, distinguishing between the northern and southern regions. A negative correlation with this component characterizes the stations located in the northern zone, suggesting a more moderate hydrological regime less

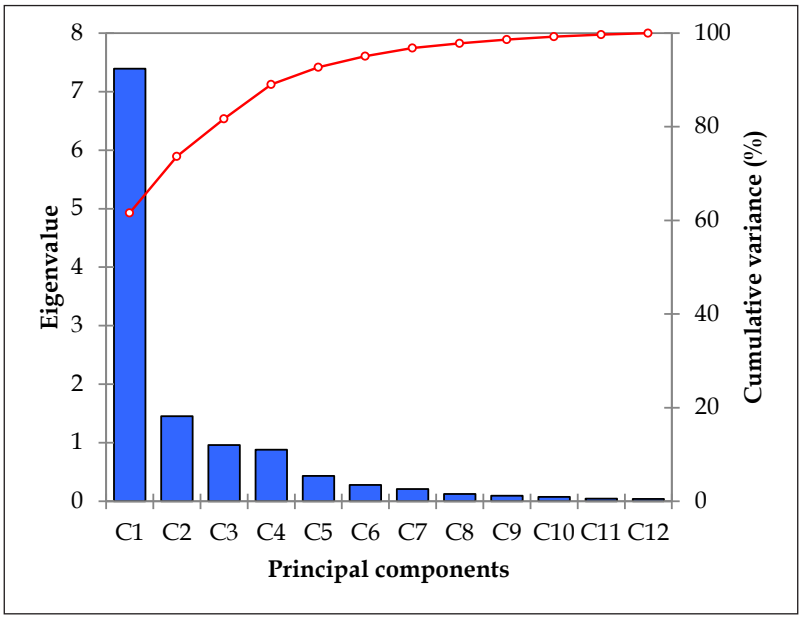

Fig. 10. Visualization of the explained and cumulative variance of the results from the Principal Component Analysis (PCA) applied to the study area.

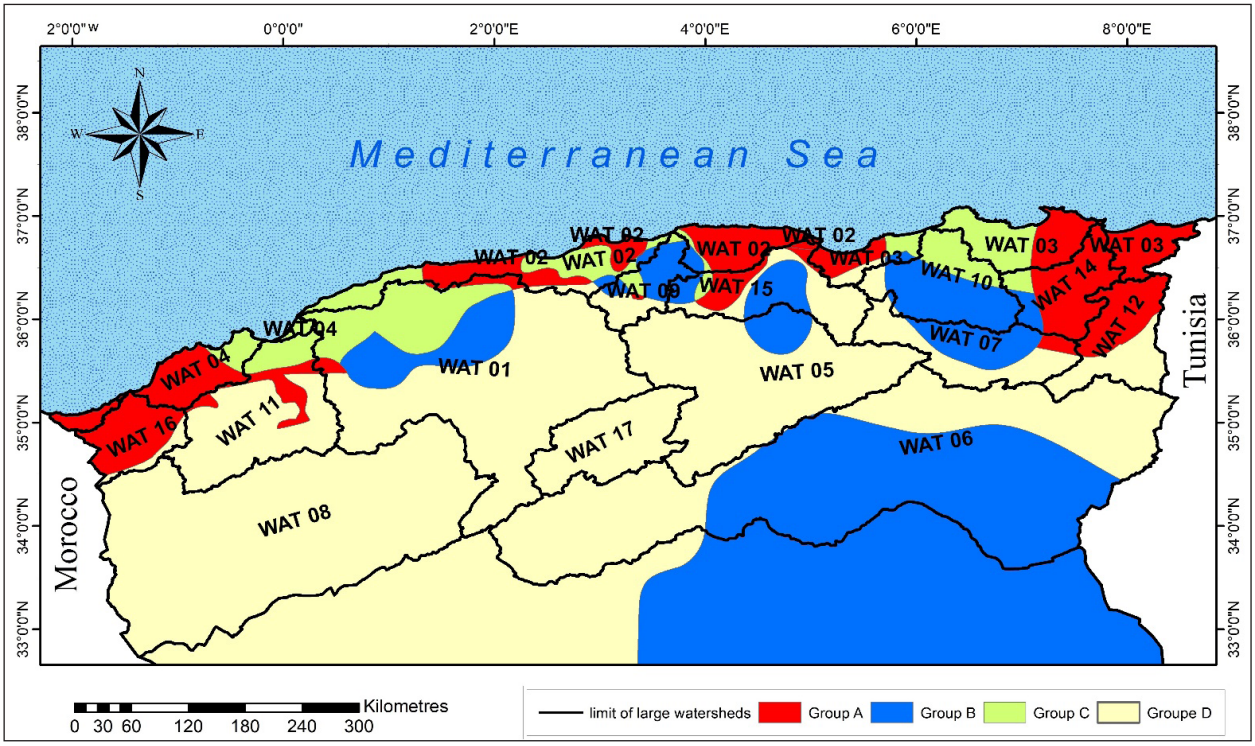

Fig. 11. Spatial distribution of the four groups identified in the study area.

prone to extreme variations. Conversely, the stations located in the southern region exhibit a positive correlation, attributable to morphological and hydrological conditions conducive to more pronounced and fluctuating sedimentary dynamics. This differentiation could be attributed to the hydrological and morphological contrasts between the Northern and Southern regions.

This differentiation, both temporal and spatial, offers an opportunity to analyze and classify the stations into four distinct categories, each reflecting specific characteristics according to the temporal and geographical dimensions. Figure 11 illustrates the spatial distribution of the different highlighted groups.

Group A includes the stations showing a negative correlation with C1 and C2. These stations record relatively low interannual sediment fluxes and are subject to a moderate hydrological regime, without significant flow fluctuations. They are mainly located in the coastal areas of the northwest and northeast.

Group B includes stations showing a positive correlation with C1 and C2. These stations are characterized by high rates of solid transport and substantial hydrological variability, reflecting marked seasonal variations. They appear in the form of scattered pockets within the territory, often in transitional zones between coastal basins and inland plains, as well as in certain southern regions.

Group C includes stations showing a positive correlation with C1 and a negative correlation with C2. These stations experience relatively significant solid transport, but with marked hydrological stability. They are mainly located in the northeast of the country.

Finally, group D includes stations showing a negative correlation with C1 and a positive correlation with C2. These stations record low sedimentary inputs but experience significant hydrological fluctuations. They are primarily located in the southern areas.

Multivariate approach aimed at characterizing the factors influencing specific erosion

The study of multiple regressions was conducted using the statistical software XLSTAT. Among the various formulations tested, the log-linear (Poisson) model proved to be the most representative and best suited to describe the variations in specific erosion based on the considered parameters. This choice is

Table 5. Most representative log-linear (Poisson) models selected for the four groups

Group	Type of model selected	Most representative models	Multiple regression coefficients
A	Log-linear (Poisson)	Es = Exp (5.037 + 0.048 Im + 0.018 IL + 0.043 Ce - 0.031 NDVI) /100	0.88
B		Es = Exp (2.587 + 0.464 Ce + 0.011 P + 0.443 Ig – 0,080 Le-0.056 NDVI) /100	0.94
C		Es = Exp (10.849 + 0.509 $\bar{I}$ + 0.001 Cof + 0.011 Ce – 0,056 NDVI-0.003 H5%) /100	0.93
D		Es = Exp (4.249 + 1.531 Kc + 0.043 Ce + 0.001 IL – 0,004 NDVI-0.091 Tc) /100	0.87

based on its ability to reflect the observed trends better and to offer greater precision in estimating erosion phenomena.

The most representative models identified in each group constitute an essential reference for in-depth analysis, refining the forecasts, and effectively guiding erosion control strategies. Their selection is based on rigorous scientific criteria, ensuring reliable and actionable results in practical applications. The main models selected for each group are summarized in Table 5.

Es: Specific erosion (t ha^{-1} yr^{-1}); Im: Average slope of a watershed (%); IL : Lithology Index, representing the percentage of shale mixed with limestone and clay with argillites (%); Ce: Runoff coefficient (%), the ratio expressed as a percentage between the amount of water drained and the amount of precipitation; NDVI: Normalized Difference Vegetation Index (%), calculated using ArcGIS software from ETM+ sensor images on the Landsat 7 satellite and OLI and TIRS sensor images on the Landsat 8 satellite; P: Average annual precipitation (mm); Ig : Overall slope index (%); Le : Average interannual water runoff (mm); $\bar{I}$: Average slope of the main watercourse (%); Cof : Fourier orographic coefficient (m^2/km^2), defined as half the difference in elevation between the highest and lowest points within the watershed, squared and divided by the watershed area; H5% : Altitude corresponding to 5% of the total surface area (m), derived from the hypsometric curve; Kc : Compactness index, calculated by comparing the perimeter of the watershed to that of a circle with the same surface area; Tc : Time of concentration (h), defined as the time required for the most distant water particle in the watershed to reach the outlet. It is calculated using the Giandotti formula.

The models resulting from the stepwise regression analysis were exponential models for all four groups, with regression coefficients of 0.88, 0.94, 0.93, and 0.87 for groups A, B, C, and D, respectively. These models are composed of independent variables that vary by group, with specific erosion (t ha^{-1} yr^{-1}) as the dependent variable. A significant correlation was observed between specific erosion and several parameters, depending on the group: it is directly proportional to the runoff coefficient, average annual precipitation, lithology index, Gravelius index, average watershed slope, overall slope index, and the Fournier orographic coefficient. Conversely, it is inversely proportional to the normalized difference vegetation index (NDVI), the altitude corresponding to 5% of the total surface area, and the time of concentration.

The average slope of a watershed (Im) plays a crucial role in the intensity of erosion, as it directly influences the speed and volume of runoff. The steeper the slope, the faster the water flows, thereby increasing its erosive power and its capacity to transport sediments. This acceleration of the water flow limits the infiltration of water into the soil, reinforcing surface runoff. This phenomenon intensifies erosion, which is manifested in particular by rill erosion, the formation of channels, and the transport of fine particles downstream. Thus, although slope is a key factor in erosion, its effect is modulated by environmental and anthropogenic elements influencing the dynamics of sediments and water within the watershed.

The lithological index (IL), which takes into account the proportion of schists associated with limestones, clay, and claystones, constitutes an essential indicator of soil sensitivity to water erosion. Indeed, the nature and composition of geological formations directly influence the stability of the terrain and their response to weathering and sediment transport phenomena. Shales and mudstones are often fissile and fragile rocks, which

makes them sensitive to physical and chemical weathering. They easily disintegrate under the action of runoff and freeze-thaw cycles, thus promoting erosion. Clay soils have low permeability, which promotes surface runoff rather than infiltration. This process amplifies water erosion, particularly in the form of rill erosion and the transport of fine particles. Although limestone may be more resistant to physical erosion, it is vulnerable to chemical erosion, particularly through dissolution in the presence of acidic water. When associated with schists, the degradation of the schist parts can accelerate the erosive process. The higher this index, the more significant the erosion, especially under conditions of heavy rainfall and steep slopes.

The runoff coefficient (Ce), is the ratio of runoff to rainfall, constitutes a key indicator in the study of water erosion. It is directly proportional to water erosion: the higher the runoff coefficient, the greater the erosion. Indeed, a high coefficient means that a large portion of the precipitation turns into runoff instead of infiltrating the soil, thus promoting the detachment and transport of soil particles. Conversely, a low runoff coefficient reduces water erosion as a larger proportion of the water infiltrates, thereby limiting runoff and sediment transport.

There is a direct proportional relationship between the average annual precipitation (P) and water erosion (Tufekcioglu *et al*., 2024). Indeed, the higher the average annual precipitation, the greater the potential for water erosion. The intensification of surface runoff explains this phenomenon due to abundant and intense precipitation. When the rainwater exceeds the soil's infiltration capacity, it generates surface runoff that exerts a mechanical force on the soil particles, causing their detachment and transport. Water erosion is all the more pronounced in regions where precipitation is not only abundant but also concentrated over short periods, which accentuates the runoff phenomenon and increases the erosive power of water.

The average annual runoff (Le) plays an essential role in the process of water erosion. In general, there is a proportional relationship between the amount of runoff water and the intensity of water erosion. The higher the runoff water depth, the greater the potential for water erosion. This phenomenon is explained by the fact that runoff water exerts a mechanical force on soil particles, causing their detachment and transport. When the volume of runoff water is significant, the erosive power of the runoff intensifies, leading to increased sediment mobilization and faster soil degradation.

The average slope of the main watercourse (Ī) is frequently identified as a determining parameter that impacts the extent of water erosion. Indeed, the steeper the slope, the greater the water flow velocity, thereby increasing its capacity to mobilize and transport soil particles. This dynamic is explained by the fact that a steeper slope generates a faster flow, amplifying the impact of the current on the banks and the riverbed. This phenomenon promotes both vertical erosion (deepening of the bed) and lateral erosion (widening of the banks), leading to a gradual modification of the river's course.

The Fournier orographic coefficient (Cof), defined as the squared half-range of elevation divided by the watershed area, is strongly associated with water erosion processes. A high coefficient, typically found in steep and rugged terrains, leads to faster and more concentrated runoff, increasing the detachment and transport of soil particles. This enhances erosion intensity and sediment yield. Its integration into predictive models significantly improves erosion risk assessment, particularly in mountainous watersheds (Tabarestani *et al*., 2022).

The overall slope index (Ig), which reflects the average inclination of a watershed, is directly related to the intensity of water erosion. Higher Ig values indicate steeper slopes, which lead to accelerated runoff and enhance the water's ability to detach soil particles. Indeed, the slope is one of the most decisive topographical factors in this process: it reduces infiltration time, increases runoff speed, and promotes sediment transport (Morgan, 2005).

The Gravelius coefficient (Kc), an indicator of the shape of a watershed, influences runoff and, consequently, water erosion. A high Kc, associated with a compact shape, promotes rapid runoff and intense flow peaks, thereby increasing the risk of erosion. This relationship was confirmed in the Wadi Mina basin,

where areas with high Kc values exhibit more pronounced erosion (Achite *et al*., 2025**)**. However, it cannot be considered directly proportional to erosion, as several other factors significantly come into play. A rounded basin (index close to 1) promotes a rapid concentration of flows, leading to more intense floods and localized but more pronounced erosion over a short period. In contrast, an elongated basin (index greater than 1) distributes the runoff over a more extended period, limiting immediate flood peaks. However, this prolonged runoff dynamic can exacerbate erosion in the long term, particularly on extensive slopes and steep inclines. Thus, although the compactness index can provide indications of the distribution of flows and their effect on erosion, it cannot be considered a unique proportional factor. Its influence must be analyzed in relation to slope, vegetation, soil type, and precipitation intensity to obtain an accurate assessment of the risk of water erosion.

The concentration time (Tc), defined as the time it takes for water from the most distant point of a watershed to reach the outlet, is an essential parameter in the analysis of runoff and water erosion. A short Tc leads to rapid runoff, high flow velocity, and increased erosion intensity. Conversely, a longer Tc promotes increased infiltration and flow dispersion, thereby reducing sediment transport. According to Amatya *et al*. (2015), the reduction of Tc significantly increases the runoff volume and erosive potential, particularly in small urbanized watersheds.

The shape of the hypsometric curve significantly influences several geomorphological factors, particularly water erosion and the age of the watershed. A young watershed, still little affected by erosion, generally presents a convex hypsometric curve. This means that the majority of its surface is located at high altitudes, reflecting a marked relief with steep slopes and minimal terrain degradation. As erosion progresses, the basin evolves, and the hypsometric curve tends to become concave gradually. In an older basin, a larger portion of the surface is found at lower altitudes, revealing a progressive leveling of the relief under the influence of erosion and sediment transport processes. This transformation is indicative of advanced erosion, having reduced topographic contrasts and gradually flattening the terrain. The H5% altitude (altitude corresponding to 5% of the total basin area) is a key indicator of this state of evolution. It is inversely proportional to the intensity of water erosion. In a young basin, where erosion remains limited, H5% is high, characterizing a rugged relief dominated by high altitudes. Over time, under the effect of erosion, the basin gradually flattens, leading to a decrease in H5%. This phenomenon is particularly pronounced in mature basins, where the slopes have been largely eroded, and the transported materials have accumulated in the low-lying areas.

The normalized difference vegetation index (NDVI) is an index calculated from satellite imagery, based on the difference in reflectance between red and near-infrared light. It allows for the assessment of the density and condition of vegetation cover. As such, the NDVI plays an essential role in reducing water erosion as an indirect indicator of vegetation cover (Amara *et al*., 2024). The relationship between NDVI and water erosion is inversely proportional: the higher the NDVI, the less pronounced the erosion, and vice versa. A high NDVI indicates dense vegetation cover, which protects the soil from the direct impact of raindrops. This cover reduces the detachment of soil particles, thereby limiting runoff and slowing down the erosion process. Moreover, vegetation promotes water infiltration by slowing down surface runoff and increasing soil porosity through its root system. A decrease in runoff leads to a reduction in sediment transport, thereby helping to limit erosion. Moreover, the root systems of plants, particularly those of herbaceous plants and shrubs, strengthen soil cohesion by stabilizing particles, thereby reducing their transport by water.

Measures are used to evaluate the accuracy and suitability of these models to the recorded data to ensure the performance of the resulting models. We employed two criteria: the coefficient of determination (R^2), the widely used Nash-Sutcliffe coefficient (Nash), and the Fisher-Snedecor test (F_{obs}) (Table 6).

In the four groups, the coefficient of determination is significantly higher than 0.7, approaching the maximum value of 1. It is situated within a range of 0.82 to 0.91, which indicates an excellent fit of the data. The Nash

Table 6. model performance indicators

Group			A	B	C	D
Criteria	Coefficient of determination (R^2)		0.85	0.90	0.91	0.82
	Nash-Sutcliffe	Nash (%)	84.71	90.41	90.92	82.35
		Simulation quality	The model is very good	The model is excellent	The model is excellent	The model is very good
Fisher-Snedecor test	F (obs)		45.20	12.95	16.06	12.00
	F (0.99)		4.16	5.99	5.04	4.31

and Sutcliffe criterion, or simply the Nash criterion, varies from 82.35% to 90.92% in this case. For groups A and D, its value is between 80% and 90%, indicating that the obtained models are perfect. As for groups B and C, the value of the criterion is above 90%, which indicates the excellence of the models obtained. For the Fisher-Snedecor test, the calculations show that F (obs) is always greater than F (0.99) for the four groups at a confidence level of 1%, which means that the models are significant.

Mapping of specific erosion in the northern part of Algeria

Natural Neighbor interpolation is a non-parametric, local interpolation method that estimates values based on weighted averages of neighboring observations within a Voronoi diagram, without extrapolating beyond the range of the observed data (Ledoux and Gold, 2005). In the context of specific erosion mapping, this method was favored due to several factors related to the characteristics of the data and the specific requirements of the project . It allows for the efficient management of a large number of observations, particularly the 123 hydrometric stations while ensuring the preservation of observed values to guarantee the reliability of the results. Its ability to handle irregular data and its accuracy in high data density areas make it an optimal choice for erosion mapping. Moreover, its non-parametric nature ensures a reliable and robust estimation of missing values, which is essential for this type of geospatial analysis.

Figure 12 illustrates specific erosion in the northern region of Algeria. It clearly highlights a north-south gradient of specific erosion in Algeria, showing very varied areas in terms of erosion intensity, ranging from low in the south and desert areas to extremely high in the Tell Mountains and certain coastal regions, where degradation often exceeds 20 t ha^{-1} yr^{-1} .

The east-west gradient, although less pronounced than the north-south gradient, highlights a significant variation in soil degradation. The areas located in the east, near the Tunisian border, generally exhibit higher levels of degradation, while those in the west, near the Moroccan border, show lower rates. In the west, regions like Tlemcen and Sidi Bel Abbès experience very low erosion, while Oran and Mascara suffer from more pronounced erosion. In the east, regions such as Constantine, Annaba, and Guelma face moderate to severe erosion, particularly in mountainous areas. Finally, in the center, erosion varies from low to very high, even extreme, with particularly vulnerable areas such as Chlef, Boumerdès, and Blida, where mountainous and urban areas require specific management and conservation measures.

Soil erosion areas in Algeria vary considerably depending on their geographical location, topography, and climate. Analyzing the different degrees of degradation allows for a better understanding of the area's most vulnerable to erosion and the identification of appropriate management strategies.

Extreme erosion zones (> 30 t ha^{-1} yr^{-1}): The areas most exposed to severe erosion are mainly located around the mountainous massifs in the northern part of the country. Among them, certain areas of Chlef, Boumerdès, Blida, and El-Tarf experience particularly intense erosive phenomena. The mountainous terrain, often steep and dotted with abrupt slopes, accentuates the vulnerability of these areas to water erosion. Indeed, the heavy seasonal rainfall, combined with the slope of the terrain, promotes rapid water runoff, thereby causing accelerated erosion, particularly in the watersheds where the intensity of water flows increases significantly. The lack of sufficient vegetation cover and inappropriate soil management exacerbate this situation, making

these areas particularly sensitive to the risks of soil degradation and loss of fertility.

Very high erosion zones (15 to 30 t ha^{-1} yr^{-1}): Very high erosion zones are spread across several regions of the country, particularly affecting Tipaza and Mila, which are completely impacted. Moreover, a large portion of the regions of Blida, Chlef, Algiers, Sétif, and Aïn-Defla also experience high levels of erosion. A significant portion of the regions of Relizane, Boumerdès, Béjaïa, Constantine, and Jijel are facing severe erosive phenomena. Some areas of Tissemsilt, Mostaganem, Oum El Bouaghi, Skikda, and Aïn-Defla are also affected by this issue.

These regions, characterized by mountainous or hilly terrain, receive relatively abundant precipitation. However, they frequently suffer from degraded or insufficient vegetation cover. This vegetation deficiency promotes surface runoff, thereby exacerbating soil degradation.

High erosion zones (5 to 15 t ha^{-1} yr^{-1}): High erosion zones are mainly located in the transition areas between mountains and coastal plains. Among these areas, Bordj-Bou-Arreridj is entirely affected by severe erosion. Other regions also experience significant erosion over vast areas, such as El-Tarf, Guelma, Annaba, Oum El Bouaghi, Khenchela, Batna, Bouira, Skikda, Relizane, Tissemsilt, M'Sila, Aïn-Témouchent, Oran, Mascara, and Mostaganem. Some smaller areas in the regions of Jijel, Constantine, Béjaïa, Tizi-Ouzou, Boumerdès, Médéa, Algiers, Sétif, and Aïn-Defla are also affected. These areas have varied terrain, with less pronounced slopes than in mountainous regions, but they remain particularly vulnerable to erosion. This situation is exacerbated by climate change and inappropriate agricultural practices.

Moderate erosion zones (2 to 5 t ha^{-1} yr^{-1}): These areas are mainly located in plain regions or areas with relatively flat terrain. They notably cover vast areas in the regions

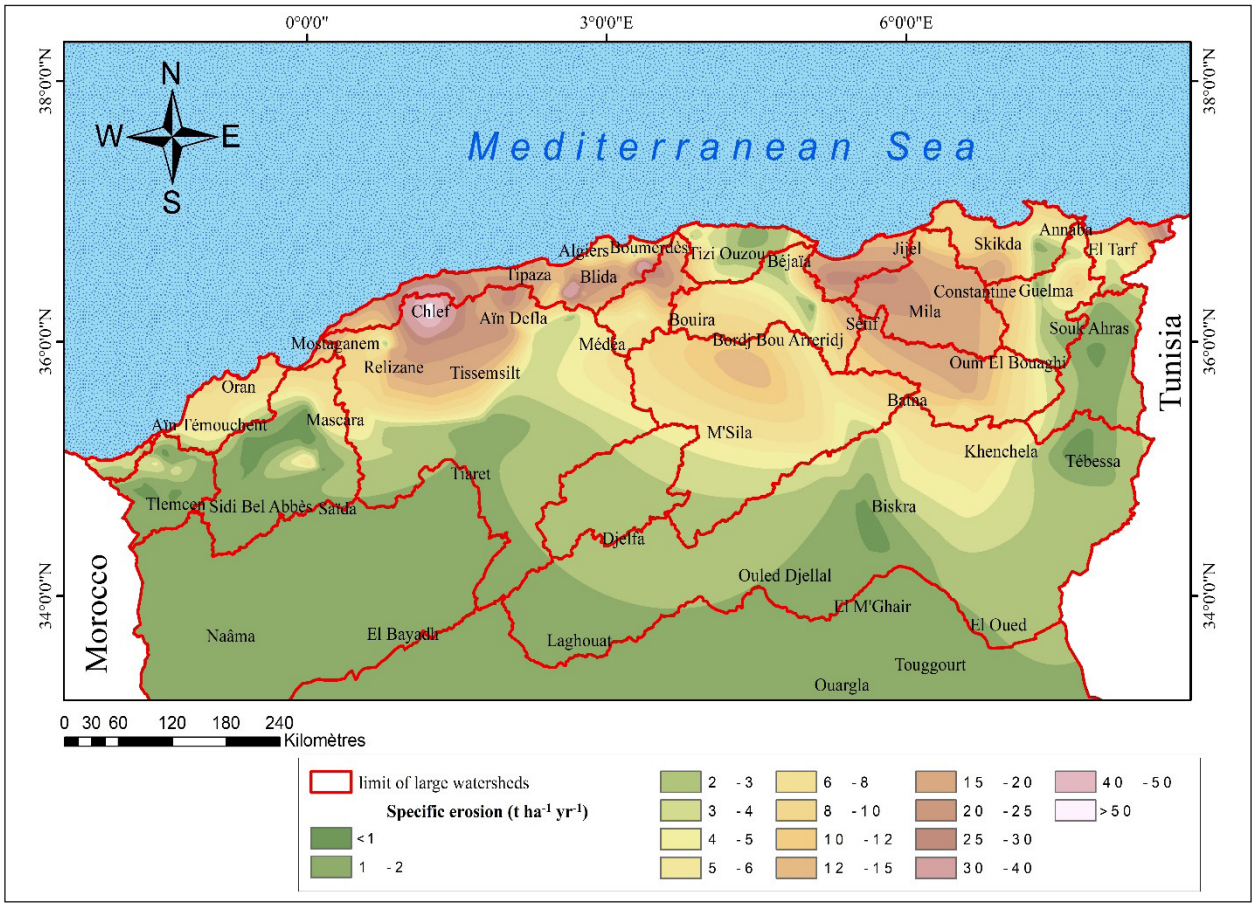

Fig. 12. Specific erosion (t ha^{-1} yr^{-1}) in northern Algeria.

of Souk-Ahras, Tébessa, El-Oued, Khenchela, Biskra, Batna, M'Sila, Djelfa, Tiaret, Médéa, and Tizi-Ouzou. Some areas, although smaller in size, are also affected, such as Guelma, Annaba, El-Tarf, Tissemsilt, Mascara, Saïda, Sidi-Bel-Abbès, Tlemcen, and Laghouat.

Annual precipitation is generally moderate in these plains and low-relief regions. However, the less pronounced topography slows down the speed of water flow, which limits the intensity of erosion compared to mountainous areas. Consequently, these regions experience moderate erosion, with less significant but still notable soil loss.

Low erosion zones (1 to 2 t ha^{-1} yr^{-1}): The areas least affected by erosion are mainly located in the southern part of the country, particularly in the steppe and arid regions. This includes all the territories of Touggourt, El M'Ghair, Ouargla, Naâma, El-Bayadh, as well as a large part of the regions of Souk-Ahras, Laghouat, Tébessa, El-Oued, Biskra, Ouled Djellal, Saïda, Sidi-Bel-Abbès, Tlemcen, and a small portion of Mascara. These regions benefit from low annual rainfall and relatively flat terrain, two factors that limit the risks of water erosion. Moreover, the vegetation, generally well adapted to arid climatic conditions, plays a crucial role in stabilizing the soils and protecting them against erosion.

Zones with very low erosion (<1 t ha^{-1} yr^{-1}): Very low erosion zones manifest as small scattered pockets in limited regions of the territory, occupying relatively small areas, often considered marginal on a national scale. Among the regions concerned are Biskra, Tébessa, Sidi Bel Abbès, Mascara, Guelma, and Tlemcen. These areas are generally located in terrains less exposed to erosive factors, such as plains or territories protected by natural elements, like dense vegetation or stable geological formations. Moreover, certain sustainable agricultural practices, such as integrated land management and the reduction of chemical inputs, play a key role in preserving soil structure and limiting erosion. These approaches significantly contribute to maintaining soil stability, thus explaining their low level of degradation.

This classification of areas based on the intensity of erosion allows for the targeting of conservation and land management efforts. Sustainable soil management, conservation agriculture, and the protection of vulnerable areas are key strategies to limit the impact of erosion and preserve the country's natural resources.

Conclusions

This study contributes to the advancement of knowledge in hydrology, particularly in the modeling and mapping of water erosion. We hope that the collection of additional data will allow us to refine and correct our results. The developed approach offers a valuable tool for predicting and managing erosion risks in Algerian watersheds.

Given the observed temporal and spatial variability, targeted and specific management for each watershed is crucial for more effective water and land management strategies. Future research should focus on improving data quality and extending models to other regions of Algeria by integrating additional variables such as land use changes and climate scenarios. This will enhance the understanding of erosion dynamics and optimize management practices for sustainable development.

References

Achit, M. and Meddi, M. 2005. Variabilité spatio-temporelle des apports liquide et solide en zone semi-aride : cas du bassin versant de l'oued Mina (nord-ouest algérien). Revue Science de l'Eau., vol. 18, n° spéciale, pp. 37-56. https://doi.org/10.7202/705575ar.

Achite, M., Djebbar, R., Meddi, M. and Dahmani, A. 2025. Mapping Soil Erosion Potential in Algeria's Wadi Mina Basin. *Sustainability* 17(11) : 5038. https://doi.org/10.3390/su17115038.

Amara, T., Saidi, F., Houhou, M.N. and Toumi, S. 2024. Relation between the soil erosion cover management factor and vegetation index in semi-arid basins. *nvironmental Earth Sciences* 83(3), Article 11593. https://doi.org/10.1007/s12665-024-11593-3.

Amatya, D.M., Cupak, A. and Wałęga, A. 2015. Influence of time of concentration on variation of runoff from a small urbanized watershed. *Geomatics, Landmanagement and Landscape* 2015 no. 2, pp. 7–19. https://doi.org/10.15576/GLL/2015.2.7.

Amatya, D.M., Skaggs, R.W. and Chescheir, G.M. 2015. Effects of time of concentration on runoff and peak flows for a drained forested watershed. *Hydrological Processes* 29(20): 4380-4394. https://doi.org/10.1002/hyp.10463.

Aouadj, S., Degdag, H., Hasaoui, O., Nasrallah, Y., Zouidi, M., Allam, A., Belkacm, N. and Khatir, H. 2023. Contribution of GIS and remote sensing for the risk mapping of soil water erosion at Saida province (Western Algeria). *Advanced Research in Life Sciences* 7(1): 10-21. https://doi.org/10.2478/arls-2023-0002.

Asselman, N.E.M. and Middelkoop, H. 2003. Impact of climate and land use change on river discharge and the production, transport and deposition of fine sediment in the Rhine basin – a summary of recent results. In: *Soil Erosion and Sediment Redistribution in River Catchments: Measurement, Modelling and Management* (Eds. J. Boardman and J. Poesen). Lecture Notes in Earth Sciences, vol. 101, pp. 163-175. Springer. https://doi.org/10.1007/3-540-36606-7_9.

Benkhaled, A. and Remini, B. 2003. Variabilité temporelle de la concentration en sédiments et phénomène d'hystérésis dans le bassin de l'Oued Wahrane (Algérie). *Hydrological Sciences Journal* 48(2): 243-255. https://doi.org/10.1623/hysj.48.2.243.44698.

Bensekhria, A. and Bouhata, R. 2023. Assessment and mapping soil water erosion using RUSLE approach and GIS tools: Case of Oued el-Hai watershed, Aurès West, Northeastern of Algeria. *ISPRS International Journal of Geo-Information* 11(2): 84. https://doi.org/10.3390/ijgi11020084.

Bouanani, A. 2004. Hydrology, solid transport and modelling study of some sub-basins of the Tafna (NW - Algeria). Doctorate thesis. University of Abou Bekr Belkaid, Tlemcen, Algeria, 249 p.

Bouanani, A., Baba Hamed, K. and Fandi, W. 2013. Production et transport des sédiments en suspension dans l'oued Sikkak (Tafna – nord ouest Algérie). Revue des Sciences de l'Eau / *Journal of Water Science* 26(2) : 119-132. https://doi.org/10.7202/1016063ar.

Bourouba, M. 1997. Les variations de la turbidité et leurs relations avec les précipitations et les débits des oueds semi-arides de l'Algérie orientale. *Bulletin ORSTOM* 17: 345–360.

Chaïeb, F., Bouderbala, A. and Hamoudi, A.S. 2024. Soil erosion analysis with GIS: A case study of Oued Sly catchment, northern Algeria. Annals of Arid Zone 63(3) : 117-123. Disponible sur : https://doi.org/10.56093/aaz.v63i3.148713.

Dagnellie, P. 1992. Théorie et méthodes statistiques. Applications agronomiques. Gembloux, Belgique, 463 p.

Demmak, A. 1982. Contribution to the study of erosion and solid transport in Northern Algeria. Thèse de doctorat d'ingénieur. Université Pierre et Marie Curie, Paris, France, 323 p.

Elahcene, O., Terfous, A., Remini, B., Ghenaim, A. and Poulet, J.P. 2013. Étude de la dynamique sédimentaire dans le bassin versant de l›Oued Bellah (Algérie). *Hydrological Sciences Journal* 58(1): 224-236. https://doi.org/10.1080/02626667.2012.742530.

FAO 2001. Soil erosion: The global picture. FAO.

FAO 2020. The state of the world's soils. FAO, Disponible sur : https://www.fao.org/3/i5199e/i5199e.pdf.

Fellah, S., Benzater, B., Guemou, L. *et al*. 2024. Using USLE, GIS and remote sensing for the soil loss assessment in the National Park of Theniet El Had, Algeria. *Journal of Agriculture and Applied Biology* 5(2): 178–193. https://doi.org/10.11594/jaab.05.02.04

Fredj, A., Ghernaout, R., Dahmani, S. *et al*. 2024. Assessing soil erosion through the implementation of the RUSLE model and geospatial technology in the Isser watershed, northern Algeria. *Water Supply* 24(7): 2487-2505. https://doi.org/10.2166/ws.2024.154.

Ghernaout, R. and Remini, B. 2017. Analyse du transport solide en suspension dans le bassin versant de l'Oued Mina (NO Algérie). La Houille Blanche 70(3) : 47-63. https://doi.org/10.1051/lhb/2017021.

JRC, 2024. Soil erosion and its economic impact. Joint Research Centre of the European Commission, https://joint-research-centre.ec.europa.eu.

Lal, R. 2001. Soil degradation by erosion. *Land Degradation & Development* 12(6): 519-539. https://doi.org/10.1002/ldr.472.

Ledoux, H. and Gold, C. 2025. An efficient natural neighbour interpolation algorithm for geoscientific modelling. In: *Developments in Spatial Data Handling*, pp. 97-108. Springer, https://doi.org/10.1007/3-540-26772-7_8.

Meddi, M. 1992. Hydro-pluviométrie et transport solide dans le bassin-versant de l'Oued Mina (Algérie). Thèse de doctorat. Université Louis Pasteur, Strasbourg, France, 285 p.

Medfouni, M.N., Korichi, K. and Marouf, N. 2024. Artificial Neural Networks vs Long Short-Term Memory Prediction of Solid Flow in Tafna Basin (North-West Algeria). *Ecological Engineering & Environmental Technology* 25(3): 275-286. https://doi.org/10.12912/27197050/181208.

Megnounif, A., Terfous, A. and Bouanani, A. 2003. Production et transport des matières solides en suspension dans le bassin versant de la Haute Tafna (Nord Ouest algérien). Revue des sciences de l'eau. 16(3) : 369-380. https://doi.org/10.7202/705513ar.

Morgan, R. 2005. Soil Erosion and Conservation, 3e éd. *European Journal of Soil Science* 56(5): 686. https://doi.org/10.1111/j.1365-389.2005.0756f.x.

Mrad, D., Boukhari, S., Dairi, S. ***et al***. 2024. Mapping the potential for erosion gullies using frequency ratio and fuzzy analytical hierarchy process: Case study Medjerda Basin, Northeast Algeria.

Eurasian Soil Science 57(8): 1381-1397. https://doi.org/10.1134/S1064229323603530.

Oldman, L., Dregne, H.E. and Watson, R. 1991. Global Assessment of Soil Degradation. ISRIC, Wageningen, Pays-Bas.

Pimentel, D., Harvey, C., Resosudarmo, P., *et al.* 1995. Environmental and economic costs of soil erosion and conservation benefits. Science. 267(5201): 1117-1123.

Roose, E., Lal, R., Feller, C., Barthès, B. and Stewart, B.A. 2005. *Soil Erosion and Carbon Dynamics*. CRC Press. https://doi.org/10.1201/9780203491935.

Semari, K. and Korichi, K. 2023. Water erosion mapping using several erosivity factors in the Macta Basin (North-West of Algeria). *Acta Hydrologica Slovaca* 24(1): 101-112. https://doi.org/10.31577/ahs-2023-0024.01.0012.

Sogreah. 1967. Étude sur l'érosion et le transport solide en Algérie. Rapport technique. SOGREAH, Ministère de l'Agriculture, Algérie, 185 p.

Sureiman, O. and Mangera, C.M. 2020. F-test of overall significance in regression analysis simplified. *Journal of the Practice of Cardiovascular Sciences* 6(2): 116-122. https://doi.org/10.4103/jpcs.jpcs_18_20.

Tabarestani, E.S., Afzalimehr, H. and Sui, J. 2022. Assessment of annual erosion and sediment yield using the first and second Fournier methods. *Water* 14(10): 1602. https://doi.org/10.3390/w14101602.

Terfous, A., Megnounif, A. and Bouanani, A. 2001. Étude du transport solide en suspension dans l›oued Mouilah (Nord Ouest Algérien). *Revue des Sciences de l'Eau* 14 : 175-185. https://doi.org/10.7202/705416ar.

Touaïbia, B. and Achite, M. 2003. Contribution à la cartographie de l'érosion spécifique du bassin versant de l'Oued Mina en zone semi-aride de l'Algérie septentrionale. *Journal des Sciences Hydrologiques*, pp. 235–240. https://doi.org/10.1623/hysj.48.2.235.44691.

Touaïbia, B., Aidaoui, A., Gomer, D. *et al.* 2001. Quantification et variabilité de l'écoulement solide en zone semi-aride de l'Algérie du Nord. *Revue des Sciences Hydrologiques* 46(1) : 41-53. https://doi.org/10.1080/02626660109492799.

Toubal, A.K., Achite, M. and Hermassi, T. 2024. Proposal of erosion control scenarios for the reduction of soil losses in the Wadi Isser basin using the RUSLE model, northwest Algeria. Arabian Journal of Geosciences. 17: 88. https://doi.org/10.1007/s12517-024-11895-7.

Tufekcioglu, M., Zaimes, G.N., Kahriman, A. and Schultz, R.C. 2024.The relationship between erosion and precipitation and the effects of different riparian practices on soil and total P losses via streambank erosion in small streams in Iowa, USA. *Sustainability* 16(19): 8329. https://doi.org/10.3390/su16198329.

Zeggane, H. and Boutoutaou, D. 2016. Quantification and multivariate analysis of water erosion in the Mediterranean region: A case study of the Isser basin, northern Algeria. In: Technologies and Materials for Renewable Energy, Environment and Sustainability. *AIP Conference Proceedings* 1758(1): 30015. https://doi.org/10.1063/1.4959411.

Zeggane, H. 2017. Study of the hydrological behavior of watercourses in Algeria, case of the Isser watershed. Thèse de doctorat. Université de Kasdi-Merbah, Ouargla, Algérie, 184 p.

Zekri, N. and Tounkob, A. 2021. Cartographie de la vulnérabilité potentielle des sols à l'érosion hydrique dans le bassin versant de Tafna (Nord-Ouest Algérien). Revue Marocaine des Sciences Agronomiques et Vétérinaires.

Printed in December 2025